# Radioactive Genesis of Hydrogen Gas under Geological Conditions: an Experimental Study

WANG Wenqing[1], LIU Chiyang[1], ZHANG Dongdong[1,*], LIU Wenhui[1], CHEN Li[2] and LIU Wei[2]

[1]*State Key Laboratory of Continental Dynamics, Department of Geology, Northwest University, Xi'an 710069, Shannxi, China*

[2]*Fangyuan Gaoke Industrial Company, Xianyang 713199, Shannxi, China*

**Abstract:** The coexistence of hydrogen-containing materials and radioactive substances in source rocks is universal. However, research about whether the latter can radiate the former to generate hydrogen gas ($H_2$) as well as the factors controlling this process remains limited. A series of radiation experiments were conducted to address this issue. Samples were placed in sealed Pyrex glass containers and subject to cobalt ($^{60}Co$) γ irradiation and components and contents of resultant gases were analyzed using gas-chromatography. The results show that all the samples released variable amounts of $H_2$ after irradiation and that the yield($H_2$) of decane is lower than that of 3-tetradecylthiophene but higher than that of distilled water, which implies that a weaker H-X bond energy (X indicates O, C or other element) in homogeneous materials corresponds with increased yield($H_2$). The yields($H_2$) of samples decreased with the decreasing solutions concentrations in sequence from mixed salts solution, KCl solution, Yellow Sea water, oil field water, gypsum solution to distilled water. The experimental results also show that the yield($H_2$) of distilled water with montmorillonite is higher than that of distilled water with kaolinite which may be due to the larger specific surface area, ion exchange capacity and more effective energy transfer effect of montmorillonite. Meanwhile, the irradiation of oxygen- and carbon-containing materials also releases $O_2$ and $CH_4$. The production of $H_2$ via the irradiation of hydrogen-containing materials makes the involvement of exogenous $H_2$ into hydrocarbon generation possible, which can enhance the hydrocarbon volume and optimize crude oil.

**Keywords:** irradiation; hydrogen-containing materials; exogenous $H_2$; hydrocarbon generation; source rocks

E-mail: nwuzhangdd@163.com (Dongdong Zhang)

## 1 Introduction

As a renewable and sustainable solution for reducing global fossil fuel consumption and combating global warming, hydrogen is a preferred alternative fuel (Celik and Yildiz, 2017;Veras et al., 2017). Most of the current uses of $H_2$ are found as processing agent in oil refineries and in chemicals production processes (Dincer, 2012). In geology, hydrogen also plays a significant role during hydrocarbon generation in source rocks. The formation of hydrocarbons in geological environments involves the addition of H and the removal of O, N, S and other heteroatoms (Hunt, 1996), which is similar to the hydro-refining technologies in industrial applications (Zhang and Gao, 1996; Matar and Hatch, 2001; Mapiour et al., 2010; Zhang et al., 2012). Although it is traditionally thought that the organic matters provide H for hydrocarbon generation by polycondensation reactions (Tissot and

This article has been accepted for publication and undergone full peer review but has not been through the copyediting, typesetting, pagination and proofreading process, which may lead to differences between this version and the Version of Record. Please cite this article as doi: 10.1111/1755-6724.14298.

Welte, 1978), Seewald (2003) noted that the organic carbon (C) is actually oversaturated in source rocks, and provided sufficient exogenous hydrogen (inorganic origin), hydrocarbons can be continuously generated until the exhaustion of a reactive carbon source.

$H_2$ can be generated in many geologic processes, such as water-rock reaction (Kita et al., 1982; Lollar et al., 2014) and serpentinization (Coveney et al., 1987; Kelley et al., 2001; Charlou et al., 2002; Schrenk et al., 2013). $H_2$ also can derive from deep earth (Wakita et al., 1980; Sugisaki and Sugiura, 1986; Chapelle et al., 2002; Potter and Konnerup-Madsen, 2003; Li and Chou, 2015; Hu et al., 2017; Mao et al., 2017). It has been proposed that formation water can provide exogenous H for hydrocarbon generation (Wang et al., 2005; Wang et al., 2006) and radiolysis may be responsible for the high concentrations of $H_2$ found in some fluid inclusions (Dubessy et al., 1988; Rabiei et al., 2017; Richard, 2017; Chi et al., 2018). Recently, large numbers of water radiolysis experiments have been conducted to study the safety issues of the nuclear waste disposal and the production of $H_2$ as a clean energy source (Pastina and LaVerne, 1999, 2001; Le et al., 2005; Dincer, 2012; Fourdrin et al., 2013; Ortiz et al., 2016; Chupin et al., 2017). These experiments confirmed that hydrogen indeed can be generated via water radiolysis and different types of irradiation have different effects on the yield of $H_2$. Additionally, the additions of some ions or minerals can promote the yield of $H_2$.

It is worth noting that oil and gas reservoirs, coal fields and uranium (U) deposits often occur within the same sedimentary basins worldwide (Li, 2000; Gan et al., 2007; Liu et al., 2007, 2016; Cai et al., 2015), especially in the Central-East Asian Multi-Energy Minerals Metallogenetic Domain (C-EAMD). Peripheral provenance areas within the C-EAMD contain abundant U-rich felsic rocks of Paleozoic and Mesozoic ages, which provide the U sources for the formation of typical sandstone-type U deposits in the adjacent basins (e.g. the Dongsheng and the Shihongtan U Deposit) and U-rich sedimentary rocks that served as hydrocarbon source rocks (Liu and Wu, 2016; Wang et al., 2018). Taking the Chang 7 Member source rocks of the Triassic Yanchang Formation in the Ordos Basin as an example, the average U content in the source rocks is up to 50 ppm (Tan et al., 2007; Qiu, 2011). There are large amounts of radioactive U and different kinds of hydrogen-containing substances (including free water, lattice water such as in $CaSO_4.2H_2O$, organic matters) in the source rocks. Numerous radiant energy produced by U decay may act on hydrogen-containing substances to generate significant volumes of $H_2$.

Although large amounts of work have been done on water radiolysis, there are still some unanswered questions. For example, it is unclear whether lattice water can release $H_2$ under irradiation. It is also uncertain what effects the dissolved materials (mainly sodium, potassium, calcium and magnesium salts) in formation waters may have on the yield of $H_2$ in rocks rich in organic matter. In order to solve these problems, a series of hydrogen-containing substances were selected for radiolysis experiments in this study, using $^{60}Co$ as the $\gamma$ radiation source. The components and contents of resultant gases after irradiation were analyzed using gas-chromatography. The results are used to evaluate the factors that may have controlled the yield($H_2$) in geologic conditions and the significance for hydrocarbon generation in sedimentary basins.

## 2 Samples and methods

The samples used in our experiment are listed in Table 1. We selected suitable samples by considering the form of hydrogen-containing substances within source rocks, and utilized distilled water alongside gypsum ($CaSO_4.2H_2O$), decane, 3-tetradecylthiophene and pitch as experimental proxies. Distilled water was used as a proxy for free water in source rocks, while gypsum represents lattice water and other compounds are typical organic matters (i.e. alkanes, heteroatom-containing compounds and solid complex mixtures). In order to capture the possible factors that influence yield($H_2$), we also utilized a range of different salt solutions (NaCl, KCl, $CaCl_2$ and $MgCl_2$) as well as Yellow Sea water, Weihe River water and a sample of oil field water. Although these latter three samples were all field-collected and comprise complex mixtures which may contain some solid impurities, they were nevertheless utilized in order to allow us to discuss the effects of salinity on yield($H_2$) semi-quantitatively. Besides, montmorillonite, kaolinite and gypsum were added to distilled water to enable discussion of the influence of the addition of the solids on the yield($H_2$). All samples were mixed with triple distilled water apart from samples of 3-tetradecylthiophene, decane, gypsum2, Yellow Sea water and Weihe River water. All samples were then placed into sealed Pyrex glass ampules (2 cm by 10 cm for 10 g 3-tetradecylthiophene, and 6 cm by 10 cm in all other cases). Samples were sufficiently outgassed and subsequently filled with approximately 1 bar of high purity He (99.999% purity) and this operation was repeated three times before all glass ampules were immediately fusion sealed. The sample of distilled water 1 was filled with air.

**Table 1 Compositions of samples and filled gas used in the experiments**

| Sample | Filled Gas | Sample Composition | Purity |
|---|---|---|---|
| 3-tetradecylthiophene | He | 10 g 3-tetradecylthiophene | 98 |
| Decane | He | 100 ml decane | 98 |
| $MgCl_2$ salt solution | He | 21.6 g Mg + 130 ml DW (14% salinity) | 99 |
| NaCl salt solution | He | 21.6 g Na + 130 ml DW (14% salinity) | 99.8 |
| KCl salt solution | He | 21.6 g K + 130 ml DW (14% salinity) | ≥99.99 |
| $CaCl_2$ salt solution | He | 21.6 g Ca + 130 ml DW (14% salinity) | 99.99 |
| Mixed salt solution | He | 0.34 g K + 11.35 g Na + 24.75 g Ca + 5.287 g Mg + 130 ml DW (24% salinity) | — |
| Pitch | He | C: 80.44%; H: 9.04%; O: 2.36%; N: 0.97%; | — |
| Oil field water | He | about 2.57% salinity | |
| Yellow Sea water | He | about 3.5% salinity | complex mixture |
| Weihe River water | He | about 0.05% salinity | |
| Montmorillonite | He | 10 g montmorillonite + 130 ml DW | — |
| Kaolinite | He | 10 g kaolinite + 130 ml DW | — |
| Gypsum1 | He | 10 g $CaSO_4 \cdot 2H_2O$ + 130 ml DW | 99% |
| Gypsum2 | He | 70 g $CaSO_4 \cdot 2H_2O$ | |
| Distilled water | He | 130 ml DW | — |
| Distilled water1 | Air | 130 ml DW+air | |

Note: K, Mg, Na, Ca and DW represent KCl, $MgCl_2$, NaCl, $CaCl_2$ and distilled water respectively; mixed salt solution is prepared following the chemical characteristics of formation water in the Ordos Basin (Li et al., 2001).

All of the samples prepared except distilled water 1 were sent to an industrial irradiator equipped with a $^{60}Co$ γ source and were subjected to a dose rate about 250Gy/h for 192 hours. The dose rate was calibrated by observing the oxidation of ferrous ions in the Fricke dosimeter using the same sample cell and configuration as in gas analysis (Pastina et al., 1999). The production of $Fe^{3+}$ was determined spectrophotometrically at 304 nm and 25 °C with an extinction coefficient of 219 $m^2$/mol and $1.61 \times 10^{-6}$ mol/J for the yield of $Fe^{3+}$. The density of 0.8N sulfuric acid was taken to be 1.022 g/$cm^3$. The absorbed dose for each sample was corrected according to its electron density.

In order to measure the relative concentrations of $H_2$, $O_2$ and $CH_4$ produced during irradiation, the gas contained in each ampule was then analyzed via gas chromatography (GC-9560-PDD) using ultra-purity He as the carrier gas. In order to quantify the amount of $H_2$ produced by irradiation, internal standard method was adopted: after measuring the relative concentration of irradiated gases, every ampule was connected with GC again, and then, 2 ml of high-purity $H_2$ was injected into ampules at 1 bar pressure condition. Followed the same steps, a new $H_2$ relative concentration was obtained via GC. According to the known content of injected $H_2$, the absolute content of $H_2$ produced during irradiation of each sample was calculated. The absolute content of $CH_4$ or $O_2$ was then obtained based on the rate of relative concentration of produced $H_2$ with that of $CH_4$ or $O_2$. Prior to the entry of irradiated gases coming into GC, a cold trap of liquid nitrogen was placed half way to eradicate any potentially produced $CO_2$, $SO_2$, $C_2H_6$, or $C_3H_8$. The detection limit is 10ppb, and the relative standard deviation is less than 1%.

## 3 Results

### 3.1 Relative concentrations of produced gas after irradiation

The gas concentration detected by GC was normalized and then the actual relative concentration of produced gas was obtained (Table 2). The results show that the relative concentrations of $O_2$ and $N_2$ in air are 21.8% and

78%, respectively. The H2 and CH4 are rare in air which is below the limit of detection,

Results show that the relative concentration of $H_2$ in distilled water without irradiation (i.e. sample of distilled water 2) was 0.054%, which is the relative concentration of $H_2$ in air. In contrast, the $H_2$ relative concentrations in samples following 192h of irradiation range between 35.85% and 95.14% (Table 2; Fig. 1); these data show that, after irradiation, different amounts of $H_2$ were indeed released from hydrogen-containing samples.

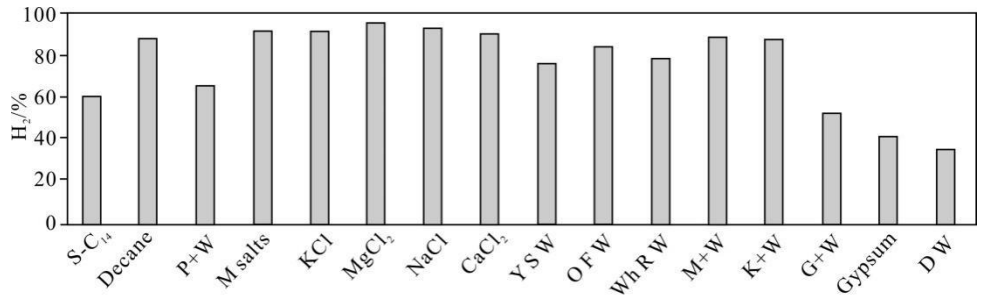


Fig. 1 Relative $H_2$ concentrations of samples after irradiation

S-$C_{14}$, 3-tetradecylthiophene; M salts, mixed salts solution; KCl, KCl solution; M+W, montmorillonite + water; Y S W, Yellow Sea water; K + W, kaolinite+water; P + W, pitch + water; O F W, oil field water; Wh R W, Weihe River water; G + W, gypsum + water; D W: distilled water with radiation (Hereinafter inclusive)

In addition to $H_2$, each sample also contains large amounts of $N_2$ which implies the residual presence of air in all cases due to incomplete vacuum-pumping. It is well-known that the ratio between $O_2$ and $N_2$ in air is about 0.28; this means that based on relative concentration of $N_2$, the $O_2$ relative concentration of residual air in each sample can be calculated (Table 2). As expected, the calculated $O_2$ relative concentrations of residual air are markedly distinct to the detected $O_2$ by GC; this means that $O_2$ was either produced or absorbed by samples during irradiation. The $O_2$ released by irradiation, is therefore defined in this analysis as the difference value (D-value) between detected $O_2$ concentration and calculated $O_2$ concentration according to $N_2$ concentration. Some D-values are positive meaning additional $O_2$ was produced and others are negative indicating the $O_2$ of air was absorbed by samples during irradiation. Meanwhile, the residual air concentration in each sample can be calculated by summing $N_2$ and $O_2$ of residual air. Besides, the concentrations of $CH_4$ in irradiated samples are higher than or comparable to that in air, implying that in some samples, such as 3-tetradecylthiophene, decane and pitch, $CH_4$ was produced.

### 3.2 $H_2$ yields produced by irradiation

Absolute yields (in mol) of $H_2$ (yields($H_2$)) were obtained using the internal standard method mentioned above and the absolute yields of $O_2$, $CH_4$ and air can be calculated according to the yield of $H_2$. In order to compare the ability of generating $H_2$ and $O_2$ under irradiation, the absolute yield per unit volume of each sample was calculated and the ratios between $H_2$ content of each irradiated sample and the $H_2$ content of distilled water with or without irradiation (Table 2).

Figure 2 is the yields($H_2$) per unit volume samples. The results of this study reveal that yields($H_2$) for different samples successively decrease in sequence from 3-tetradecylthiophene, decane, salt solutions, Yellow Sea water, pitch, oil field water, Weihe River water, $CaSO_4.2H_2O$ to distilled water. The ratios of yields($H_2$) of irradiated samples with the yields($H_2$) of irradiated distilled water range between 1.8 and 262 (Table 2). Besides,

**Table 2 Results of produced gases of samples after irradiation**

| Samples | Filled gas | Relative concentration/% | | | | | | Absolute content $*10^{-5}$/mol | | | | | Absolute content of per unit volume $*10^{-5}$/mol | | Ratio of $H_2$ content |
|---|---|---|---|---|---|---|---|---|---|---|---|---|---|---|---|
| | | $O_2$+Ar | $N_2$ | $H_2$ | $CH_4$ | $O_2$ of Residual air | Residual air | $O_2$ produced | $H_2$ | $O_2$ | $CH_4$ | Air | $H_2$ | $O_2$ | S/DW with irradiation |
| 3-tetradecylthiophene | He | 2.81 | 35.81 | 60.83 | 0.172 | 10.03 | 45.84 | -7.217 | 51.4 | -6.1 | 0.145 | 38.8 | 4.731 | -0.561 | 262 |
| Decane | He | 0.33 | 11.08 | 87.8 | 0.456 | 3.102 | 14.18 | -2.772 | 290.8 | -9.18 | 1.51 | 47 | 2.908 | -0.092 | 161 |
| Pitch | He | 1.9 | 29.99 | 65.63 | 1.953 | 8.397 | 38.39 | -6.497 | 39.1 | -3.87 | 1.16 | 22.9 | 0.301 | -0.030 | 17 |
| Mixed salt solution | He | 1.03 | 7.13 | 91.39 | 0.0017 | 1.996 | 9.126 | -0.966 | 98.5 | -1.04 | $1.84*10^{-3}$ | 9.84 | 0.758 | -0.008 | 42 |
| KCl salt solution | He | 1.58 | 6.24 | 91.77 | 0.0034 | 1.747 | 7.987 | -0.167 | 78.4 | -0.143 | $2.91*10^{-3}$ | 6.83 | 0.604 | -0.001 | 33 |
| $MgCl_2$ salt solution | He | 0.66 | 3.88 | 95.14 | 0.0025 | 1.086 | 4.966 | -0.426 | 77.8 | -0.349 | $2.11*10^{-3}$ | 4.06 | 0.599 | -0.003 | 33 |
| NaCl salt solution | He | 0.86 | 5.6 | 92.72 | 0.0020 | 1.568 | 7.168 | -0.708 | 70.6 | -0.539 | $1.55*10^{-3}$ | 5.46 | 0.543 | -0.004 | 30 |
| $CaCl_2$ salt solution | He | 3.14 | 6.5 | 90.11 | 0.0018 | 1.82 | 8.32 | 1.32 | 38.9 | 0.57 | $8.12*10^{-4}$ | 3.6 | 0.300 | 0.004 | 17 |
| Yellow Sea water | He | 14.55 | 9.37 | 76.06 | 0.004 | 2.624 | 11.99 | 11.93 | 45.8 | 7.18 | $2.41*10^{-3}$ | 7.22 | 0.352 | 0.055 | 19 |
| Oil field water | He | 9.44 | 5.91 | 84.51 | 0.008 | 1.655 | 7.565 | 7.785 | 29.9 | 2.76 | $2.83*10^{-3}$ | 2.68 | 0.230 | 0.021 | 13 |
| Weihe River water | He | 10.74 | 10.17 | 79.05 | 0.008 | 2.848 | 13.02 | 7.892 | 20.7 | 2.07 | $2.1*10^{-3}$ | 3.42 | 0.160 | 0.016 | 9 |
| Montmorillonite | He | 0.6 | 10.65 | 88.67 | 0.013 | 2.982 | 13.63 | -2.382 | 53.5 | -1.44 | $7.85*10^{-3}$ | 8.23 | 0.412 | -0.011 | 23 |
| Kaolinite | He | 0.57 | 11.2 | 88.17 | 0.012 | 3.136 | 14.34 | -2.566 | 41.5 | -1.21 | $5.65*10^{-3}$ | 6.75 | 0.319 | -0.009 | 18 |
| Gypsum1 | He | 8.51 | 38.44 | 53.02 | 0.023 | 10.76 | 49.2 | -2.253 | 9.185 | -0.39 | $3.98*10^{-3}$ | 8.52 | 0.071 | -0.003 | 4 |
| Gypsum2 | He | 5.52 | 51.73 | 42.03 | 0.191 | 14.48 | 66.21 | -8.964 | 2.301 | -0.491 | $1.05*10^{-2}$ | 3.62 | 0.033 | -0.007 | 1.8 |
| Distilled water | He | 19.58 | 44.53 | 35.85 | 0.029 | 12.47 | 57 | 7.112 | 2.351 | 0.466 | $1.9*10^{-3}$ | 3.74 | 0.018 | 0.004 | 1 |
| Air | Air | 21.84 | 78.04 | - | - | - | - | - | - | - | - | - | - | - | - |

Note: S/DW represents the rate of sample/distilled water

yields($H_2$) for different kinds of salt solutions are significantly enhanced compared to distilled water; with the yields($H_2$) gradually decreasing in sequence from mixed salts solution through KCl, $MgCl_2$, NaCl to $CaCl_2$ (Fig. 3a). The results also show that the yield($H_2$) increases with the addition of gypsum, kaolinite and montmorillonite, with the latter two being the most effective (Fig. 3b).

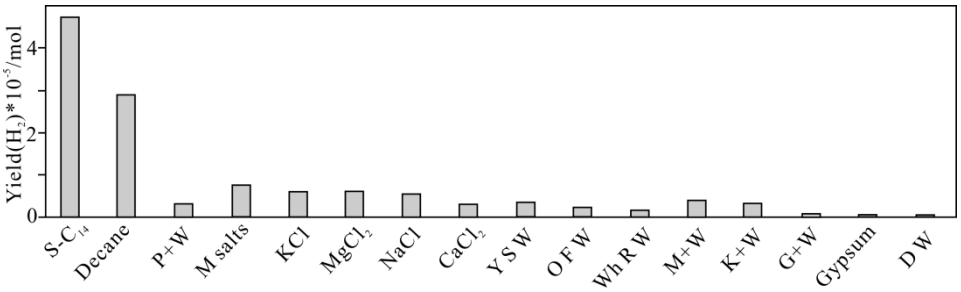


Fig. 2 Yields($H_2$) per unit volume samples under irradiation

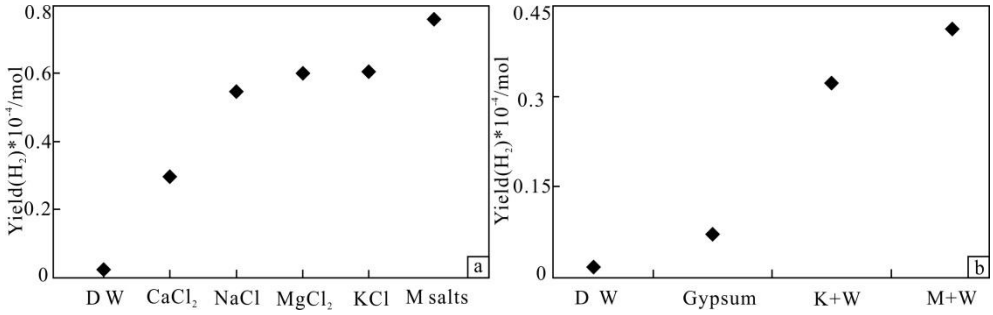


Fig. 3 Yield($H_2$) as a function of (a) different kinds of salt solutions and (b) with the addition of different minerals

### 3.3 $O_2$ Yields produced by irradiation

Based on the yield of $H_2$, the yield of $N_2$ and $O_2$ of residual air can be calculated, so is the residual air. Figure 4 shows the contents of residual air that remained in each sample. It reveals that a large volume of air remained in 3-tetradecylthiophene, decane and pitch samples; this is because the vacuum degrees were controlled at lower level in these three cases considering that the Pyrex glass ampule used in the first case measured 2 cm by 10 cm and was therefore more fragile than those used for other samples and decane is easily volatile and powered pitch can be sucked back at high vacuum degree; except for these three samples, the vacuum degrees of all other cases were higher (Fig.4).

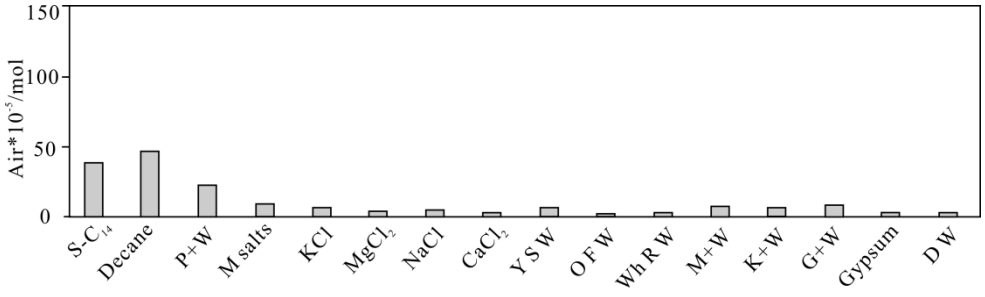


Fig. 4 The absolute residual air content of each sample

The D-value between detected $O_2$ content and $O_2$ content of residual air is the yield of $O_2$ produced by sample under irradiation (Table 2). Figure 5 is the $O_2$ produced per unit volume sample under irradiation. The results show that the yields($O_2$) of samples including 3-tetradecylthiophene, decane and pitch are significantly negative, while the yields($O_2$) of Yellow Sea water, oil field water and Weihe River water are significantly positive. At the same time, yields($O_2$) of $CaCl_2$ solution and distilled water are weakly positive while the yields($O_2$) of other samples are weakly negative (Fig.5). Organic matters containing C atoms (including 3-tetradecylthiophene, decane and pitch) all release abundant $CH_4$ (Table 2).

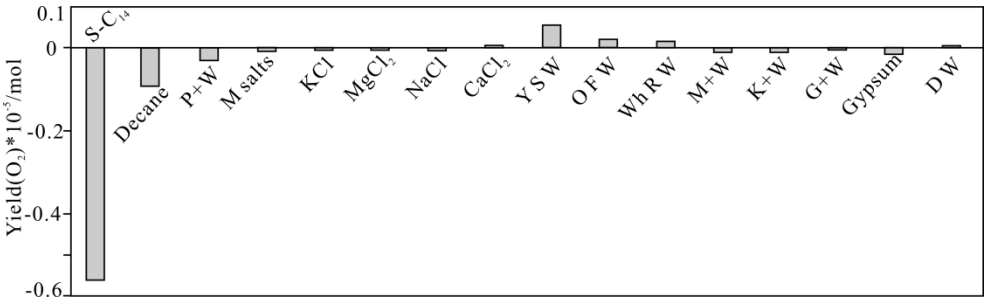


Fig. 5 Yields($O_2$) per unit volume samples after irradiation

## 4 Discussions

### 4.1 Factors controlling yields($H_2$) of samples under irradiation

#### 4.1.1 Difference in H-X (X represents O or C atom) bond energy

It is well-known that the longer the straight-chain paraffin is, the weaker its C-H bond energy; at the same time, C-C bond energy is also weaker than C-H bond energy for the same organic molecule and with the breakage of C-C and C-H bonds, the C-H bonds of $CH_3\cdot$, $CH_2\cdot$ and $CH\cdot$ are easier to break (Luo, 2005; Miao and Pang, 2012). Thus, in the case of decane, an organic molecular that comprises ten carbons, the C-H bond energy is lower than 414 KJ/mol (the C-H bond energy of heptane) and the $C_5$-$C_5$ bond energy is 360kJ/mol which are much less than the H-O bond energy of $H_2O$ (497 kJ/mol). Similarly, 3-tetradecylthiophene comprises a 14 carbons branch chain and a sulfur heteroatomic ring; in this case, the C-H bond energy of the carbon branch chain is lower than that of decane and the double bond in sulfur heteroatomic ring makes the C-H in carbon branch chain easier to break. Above all, in the same irradiation environment, 3-tetradecylthiophene will therefore release more $H_2$ than decane, while $H_2O$ will release the least which correspond to the experimental results. Pitch mainly comprises a series of aromatic rings and is the most complex mixture found within oil (Miao and Pang, 2012). The C-H bond energy of aromatic ring is 472 kJ/mol (Luo, 2005); this means that the yield($H_2$) of pitch is lower than that of decane and 3-tetradecylthiophene but higher than that of $H_2O$. The results show that the yield($H_2$) of $CaSO_4.2H_2O$ ($2.301 \times 10^{-5}$ mol) is comparable to that of $H_2O$ ($2.351 \times 10^{-5}$ mol) (Table 2). However, the yield($H_2$) per unit mass $CaSO_4.2H_2O$ is higher than that of $H_2O$ which may be because there are new bonds formed between $CaSO_4$ and $H_2O$ weakening the H-O bond energy of lattice water (Li et al., 2002) (Table 2; Fig. 6).

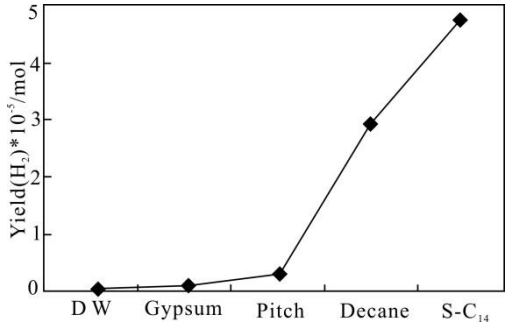


Fig. 6 Per unit mass yield($H_2$) plotted as a function of decreasing H-X bond energy

#### 4.1.2 The addition of salts and the salt types

The results show that the yields($H_2$) of salt solutions considered here (i.e. $MgCl_2$, KCl, NaCl and $CaCl_2$

solutions) are much more than that of distilled water; this implies that the addition of some salts can increase the yields($H_2$)(Fig. 3a). As salts dissolve in water, new covalent bonds will form between cations and O and between anions and H. For example, when NaCl dissolves in water, both O and H in water will combine with Na and Cl respectively (Olleta et al., 2006) and when $MgCl_2$ dissolves in water, O and H in water will connect with Mg and Cl respectively (Feng et al., 2017). The formation of new covalent bonds will weaken the H-O bond energy in water (Li et al., 2002), and reduce the energy required to rupture this bond and contribute to the generation of additional $H_2$ under irradiation.

Four salt solutions were irradiated in our experiment including KCl, $MgCl_2$, NaCl and $CaCl_2$ solutions. The yields($H_2$) of KCl, $MgCl_2$ and NaCl in this case are almost the same, close to double yield($H_2$) of $CaCl_2$ (Fig.3a) which implies that different salt types have different effects on the yield($H_2$). In this experiment, we therefore hypothesize that $Ca^{2+}$ ions exert an inhibitory or a weak stimulating effect on $H_2$ generation under irradiation.

#### 4.1.3 Salt solubility

The results show that the yield($H_2$) of $CaCl_2$ solution is much more than that of $CaSO_4 \cdot 2H_2O$ solution. The discrepancy might be due to differences between $CaCl_2$ and $CaSO_4$ in anion types and solubility. According to Feng et al. (2015), the new covalent bonds will form between O atoms in $SO_4^{2-}$ and H atoms in $H_2O$ as well as between Ca and O atoms in $H_2O$, which is similar to $CaCl_2$ dissolving in water. Above all the yields($H_2$) will mainly be affected by the solubility of $CaCl_2$ and $CaSO_4 \cdot 2H_2O$. The solubility of $CaSO_4 \cdot 2H_2O$ is 0.25 g, while the solubility of $CaCl_2$ is 74.5 g. The concentration of $CaCl_2$ in this experiment is 14%, while the concentration of $CaSO_4 \cdot 2H_2O$ is 0.25%. This means that more new covalent bonds formed in the $CaCl_2$ solution than that in the $CaSO_4 \cdot 2H_2O$ solution. Besides, yields($H_2$) of mixed salts solution, KCl solution, Yellow Sea water, oil field water as well as $CaSO_4 \cdot 2H_2O$ solution decrease successively in correspondence with the main ions (i.e. $K^+$, $Ca^{2+}$,$Na^+$, $Mg^{2+}$) content variations in sequence from mixed salts solution (24.3%), KCl solution (14%), Yellow Sea water (3.5%), oil field water (2.57%) and $CaSO_4 \cdot 2H_2O$ (0.25%) (Fig. 7). It is worth mentioning that, the yield($H_2$) of Weihe River water (0.05%) is more than that of $CaSO_4 \cdot 2H_2O$; this might be due to the presence of some solid impurities, which may enhance the yield($H_2$), as discussed below.

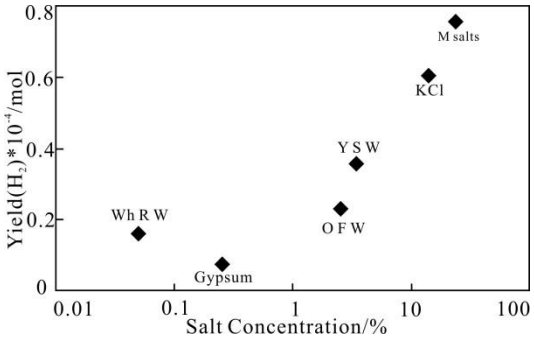


Fig. 7 Yield($H_2$) plotted as a function of the salt concentration

The Na-Cl bond will break when a NaCl molecular dissolves in nine $H_2O$ molecules (i.e. the molar ratio between $H_2O$ and NaCl is 9:1) corresponding to NaCl salinity of 26.4%, the saturation of NaCl solution in room temperature. The Na-Cl bond breaks more easily with the lower salinity. That is, when the concentration of NaCl is less than saturation solubility, favorable conditions for Na-Cl breaking will be generated (Hou et al., 2017). Previous experimental work has shown that when the Na-Cl bond breaks, there will be more $H_2O$ molecules combining with $Na^+$ and $Cl^-$ (Olleta et al., 2006). It can be inferred that when the content of NaCl reaches the saturation solubility, there will be the most covalent bonds forming corresponding to the most yield of $H_2$, which is consistent with our experiment results. Overall, according to our experimental results, the higher the concentration is, the more $H_2$ will be generated under γ irradiation.

#### 4.1.4 The addition of solid minerals and their properties

Although montmorillonite and kaolinite are insoluble in water, yields($H_2$) of both clays are much more than that for distilled water (Fig. 3b). Previous studies have shown that this is because of the energy transfer effect of solids. That is, the additions of some solids (e.g. montmorillonite, zeolite, silica gel) will multiply the yield($H_2$) of distilled water. The mechanism is that, firstly, the ionization of the irradiated solid matters leads to the production of a positive hole and an electron (Nakashima and Masaki, 1996) which can either recombine

with one another or remain trapped in the matrix. Secondly, electrons which are not trapped in solid matters can be transferred from the ionized surface to bulk water where they are hydrated via the reaction of $e^- + H_2O \rightarrow e^-_{aq}$ (Musat et al., 2012; Fourdrin et al., 2013). These hydrated electrons then cause $H_2$ production via the reaction of $e^-_{aq} + e^-_{aq} + 2H_2O \rightarrow H_2 + 2OH^-$ (Pastina et al., 1999, 2001). At the same time, water molecules will interact with the positive holes ($h^+$) because of their electron-donating properties, and so $H_2$ will be formed via the reactions of $H_2O + h^+ \rightarrow H^+ + OH$ and $H^+ + e^- \rightarrow 1/2H_2$. However, it has also shown that, at a given absorbed energy, hydrogen yield in the silica gel-water system is higher than that in the molecular sieve 5 A-water system; this phenomenon indicates that the effectiveness of energy transfer will be strongly influenced by the nature of the solid (Nakashima and Masaki, 1996).

In an early study, Chupin et al. (2017) proved that when specific surface area increased and mean pore size decreased, $G(H_2)$ (the $H_2$ yield per Joule (mol/J)) values increased linearly. The influence of specific surface area of geopolymers on yield($H_2$) might be explained by energy transfer between solid and the pore solution. The larger of the specific surface area, the more energy is transferred from a geopolymer surface to the pore solution (Frances et al., 2015). In terms of the effects of pore size on $G(H_2)$, when mean pore size decreases, a confinement effect occurs that favors the dimerization of H radicals and of hydrated electrons produced in the same pore resulting in yield($H_2$) increase (Le et al., 2005). The recombination probability for primary radical species formed within the pore solution will also be larger for smaller pores because this dimension is related to the mean free path of their diffusion, and the hydrogen formation could thus be promoted. Indeed, the specific surface area of montmorillonite in our experiment is larger than that of kaolinite, so the yield($H_2$) of montmorillonite is more than that of kaolinite.

The ion exchange capacity of montmorillonite is also stronger than that of kaolinite; in other words, more $Al^{3+}$ and $Si^{4+}$ will be replaced by divalent and trivalent ions respectively, rendering montmorillonite electronegative (Liu, 2009). Then, new covalent bonds will form between electronegative montmorillonite and H atoms in $H_2O$ weakening the H-O bond energy and lowering the activation energy required for H-O bond rupture in water which contributes to the generation of additional $H_2$ in a similar way to salt solutions. Besides, according to the recent research of Truche et al. (2018), some $H_2$ can be adsorbed by minerals and the adsorption ability of kaolinite is higher than montmorillonite. That is to say, the detected radiolytic $H_2$ of kaolinite might be far lower than that of montmorillonite sample which needs further research. We all know that $CaSO_4 \cdot 2H_2O$ is sparingly soluble, and the solubility of $CaSO_4 \cdot 2H_2O$ is 0.25g at room temperature. The yield($H_2$) of the sample consisting of 10g $CaSO_4 \cdot 2H_2O$ and 130ml distilled water is controlled by dissolved 0.325 g $CaSO_4 \cdot 2H_2O$ in 130ml distilled water and 9.675 g of solid $CaSO_4 \cdot 2H_2O$. However, the yield($H_2$) of $CaSO_4 \cdot 2H_2O$ is still lower than that of montmorillonite and kaolinite which implies that the stimulative effect of solid $CaSO_4 \cdot 2H_2O$ on the yield($H_2$) is much lower than that of montmorillonite or kaolinite (Fig. 3b).

### 4.2 The characteristics of yields($O_2$) and yields($CH_4$) under irradiation

It is also easy to understand the negative yields($O_2$) of 3-tetradecylthiophene and decane because of their lack of oxygen atoms and strong reducing properties. Figure 4 shows that the proportions of residual air in 3-tetradecylthiophene and decane samples are very high, while the yields($O_2$) of them are extremely negative; these results confirm that these two samples indeed consume large amounts of $O_2$. Additionally, although the yield($O_2$) of distilled water is positive (Fig.5), the yield($O_2$) of pitch with distilled water is negative implying that the reducing pitch consumed the $O_2$ of residual air as well as the $O_2$ produced by water irradiation. Meanwhile, it is well-known that oil field water contains some reduced liquid hydrocarbons which will consume $O_2$; in this case, however, the yield($O_2$) of oil field water remains obviously positive, meaning that the consumption of $O_2$ by reduced hydrocarbons remains much less than the generation of $O_2$ from oil field water.

Figure 8 shows the yields($O_2$) variation of samples as a function of yields($H_2$); these data show that the yields($O_2$) of organic matters (i.e. 3-tetradecylthiophene, decane and pitch) are all negative and decrease with increasing yields($H_2$). Meanwhile, the yields($O_2$) of complex mixtures (i.e. Weihe River water, oil field water and Yellow Sea water) are all undoubtedly positive and increase in concert with yields($H_2$). However, the yields($O_2$) of other samples (including distilled water with salts or solid minerals) range between $-1 \times 10^{-5}$ mol and $1 \times 10^{-5}$ mol and the relationships of yields($O_2$) and yield($H_2$) for these samples are unclear and thus further research is needed.

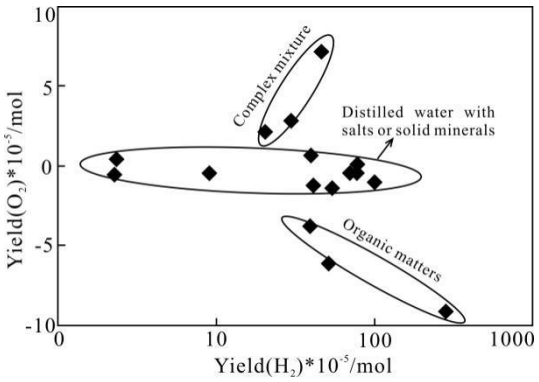


Fig. 8 Yield($O_2$) as a function of yield($H_2$)

The results also show that the organic matters release lots of $CH_4$ under irradiation (Table 1) and that the yields of $CH_4$ from 3-tetradecylthiophene and decane are more than that from pitch, perhaps because the C-C bond energy in the latter is higher than in either of the former compounds (Luo, 2005). The high bond energy makes the C-C bond rupture difficultly, thus suppressing the production of $CH_4$.

### 4.3 Geological implications

The experimental data reported here demonstrate that the hydrogen-containing materials can release $H_2$ under irradiation and the additions of salts or solid minerals into distilled water can multiply the amount of yields($H_2$). Taking the source rocks of Chang 7 member in the Ordos Basin as an example, according to the burial history of the Ordos Basin, Chang 7 member came into oil generation window in the Mid-Jurassic (170 Ma), and until now, the temperature of this member remains over 60°C (Liu and Wu, 2016). This suggests that the high-content U (about 50 ppm on average) in this member may have been providing effective radiation energy (during hydrocarbon generation period) for the source rocks in Chang 7 member since Mid-Jurassic. Calculations show that 50 ppm U within the Chang 7 member makes the source rocks to be exposed to a dose rate as high as $0.3 \times 10^{-6}$ Gy/h (Rong, 2002) since Mid-Jurassic, and so the total radiation dose in this case could be as high as $4.2 \times 10^5$ Gy (1 Gy = 1 J/kg). In other words, since 170Ma, 1 kg source rocks would have been irradiated by $4.2 \times 10^5$ J of radiation energy. The coexistence of abundant U as well as numerous kinds of hydrogen-containing substances in source rocks provides the energy and material basis for water radiolysis in the Ordos Basin.

From Chang 10 Member to Chang 7 Member, the Ordos Basin was in lake invasion period and in Chang 7 Member, the lake invasion reached the largest region (Zhang et al., 2008) and so source rocks developed in this period are rich in clay minerals such as interstratified illite/ montmorillonite, illite, montmorillonite and kaolinite (Feng et al., 2018). These minerals comprise between 18% and 37% total mass (Zhang et al., 2008) and can enhance yield($H_2$) as revealed by our experiments. Pores within Chang 7 member source rocks are microporous (10%, less than 2 nm) as well as mesoporous (77%, between 2 nm and 50 nm). Indeed, most pores are smaller than 4 nm in size (Feng et al., 2018), similar to those in Geo Cs (Chupin et al., 2017), which correspond to a relatively large specific surface areas and are thus favorable for $H_2$ generation under irradiation. The characteristics of trace elements within Chang 7 member source rocks reveal that during sedimentation and diagenetic periods, the environment was anaerobic-reducing and thus conducive for the preservation of $H_2$ from the irradiation of hydrogen-containing materials.

Provided large amounts of radiant energy, water with different ions and solids and favorable conditions provided by source rocks, abundant $H_2$ would have been released in the Chang 7 source rocks. There is a strong possibility that large amounts of exogenous $H_2$ from water radiolysis could be involved in hydrocarbon generation in actual geological environments (Seewald, 2003). The exogenous $H_2$ can react with unsaturated, long-chain hydrocarbons and sulfur or nitrogen compounds in certain temperature and pressure to produce saturated and short-chain hydrocarbons, as shown by the reactions below, which not only can optimize crude oil but also increase the quantity of oil and gas (equations 8-10; Zhang and Gao, 1996; Matar and Hatch, 2001; Mapiour et al., 2010; Dincer, 2012; Zhang et al., 2012).

$$R'CH{=}CH_2 + H_2\ (\text{catalyst}) \rightarrow R'CH_2CH_3 \quad (8)$$

$$RCH_2CH_2CH_2R' + H_2 \rightarrow RCH_2CH_3 + R'CH_3 \quad (9)$$

$$R\text{-}SH + H_2 \rightarrow RH + H_2S \quad (10)$$

$$CO_2 + 3H_2 \text{ (with microbial processes)} \rightarrow CH_4 + H_2O \quad (11)$$

Shale oil source rocks can generate hydrocarbons as well as store oil and gas. Provided elevated U concentrations in this kind of oil shale, continuous radiant energy will enable macromolecular to become micromolecular and the unsaturated hydrocarbons to become saturated hydrocarbons by reactions including hydrogenation and hydrocracking (Matar and Hatch, 2001). Furthermore, as crude oil migrates into a sandstone reservoir which is rich in U, the oil quality may be improved through the addition of exogenous $H_2$ from water radiolysis. In this context, our experiments have provided preliminary results that will stimulate new hydrocarbon generation theories.

## 5 Conclusions

(1) hydrogen-containing materials including all kinds of water and organic matters can generate large volumes of $H_2$ under γ irradiation.

(2) Generally speaking, in terms of pure materials, the smaller the H-X bond energy, the more $H_2$ can be produced.

(3) The addition of some salts can promote yield($H_2$) of water greatly and the higher the salt solution concentration is , the more $H_2$ will be generated.

(4) The presence of solid minerals in distilled water can also multiply yield($H_2$). The yield($H_2$) is proved to be affected greatly by the nature of the solids.

(5) There is a strong probability that the source rocks of Chang 7 member have released abundant $H_2$ from hydrogen-containing materials due to natural radioactive irradiation, promoting the production of hydrocarbons and optimizing the petroleum in the Ordos Basin.

## Acknowledgements

Thank the anonymous reviewers and associate editor, Chi Guoxiang, for your constructive suggestions to improve the paper. We also thank Prof. X.P. Ouyang for helpful suggestions and Dr. F. Chupin for technical assistance. This work was supported by the National Natural Science Foundation of China [Grant numbers 41330315, 41402093].

## References

Cai Y.Q., Zhang J.D., Li Z.Y., Guo Q.Y., Song J.Y., Fan H.H., Liu W.S., Qi F.C., and Zhang M.L., 2015. Outline of uranium resources characteristics and metallogenetic regularity in china. *Acta Geologica Sinica* (English Edition), 89(3): 918–937.

Çelik, D., and Yıldız, M., 2017. Investigation of hydrogen production methods in accordance with green chemistry principles. *International Journal of Hydrogen Energy*, 42(36): 23395–23401.

Chapelle, F.H., O'Neill, K., Bradley, P.M., Methe, B.A., Ciufo, S.A., Knobel, L.L., and Lovley, D.R., 2002. A hydrogen-based subsurface microbial community dominated by methanogens. *Nature*, 415: 312–315.

Charlou, J.L., Donval, J.P., Fouquet, Y., Jean-Baptiste, P., and Holm, N., 2002. Geochemistry of high $H_2$ and $CH_4$ vent fluids issuing from ultramafic rocks at the Rainbow hydrothermal field (36°14'N, MAR). *Chemical Geology*, 191:345-359.

Chi, G., Blamey, N.J.F., Rabiei, M., and Normand, N., 2018. Hydrothermal rare earth element (Xenotime) mineralization at Maw Zone, Athabasca Basin , Canada, and its relationship to unconformity-related uranium deposits-A reply. *Economic Geology*, 113: 998-999.

Chupin, F., Dannoux-Papin, A., and Ravache, Y.N., 2017. Water content and porosity effect on hydrogen radiolytic yields of geopolymers. *Journal of Nuclear Materials*, 494: 138–146.

Coveney, R.M., Goebel, E.D., Zeller, E.J., Dreschhoff, G.A.M., and Angino, E.E., 1987. Serpentinization and the origin of hydrogen gas in Kansas. *Am. Assoc. Pet. Geol. Bull.* (United States), 71: 39–48.

Dincer, I., 2012. Green methods for hydrogen production. *International Journal of Hydrogen Energy*, 37: 1954–1971.

Dubessy, J., Pagel, M., Beny, J.M., Christensen, H., Hickel, B., Kosztolanyi, C., and Poty, B., 1988. Radiolysis evidenced by $H_2$-$O_2$ and $H_2$-bearing fluid inclusions in three uranium deposits. *Geochim Cosmochim Acta*, 52: 1155–1167

Feng G., Hou G.L., Xu H.G., Zeng Z., and Zheng W.J., 2015. On the dissolution of lithium sulfate in water: anion photoelectron spectroscopy and density functional theory calculations. *Physical Chemistry Chemical Physics*, 17: 5624–5631.

Feng G., Liu C.W., Zeng Z., Hou G.L., Xu H.G., and Zheng W.J., 2017. Initial hydration processes of magnesium chloride: size-selected anion photoelectron spectroscopy and ab initio calculations. *Physical Chemistry Chemical Physics*, 19: 15562–15569.

Feng X.L., Ao W.H., and Tang X., 2018. Characteristics and main controlling factors of the formation of pores in continental shale gas reservoirs: A case study of Chang 7 Member in Ordos Basin. *Journal of Jilin University* (Earth Science Edition), 48: 678-692 (in Chinese with English abstract).

Fourdrin, C., Aarrachi, H., Latrille, C., Esnouf, S., Bergaya, F., and Le, C.S., 2013. Water Radiolysis in Exchanged-Montmorillonites: The $H_2$ Production Mechanisms. *Environmental Science & Technology*, 47: 9530–9537.

Frances, L., Grivet, M., Renault, J.P., Groetz, J.E., and Ducret, D., 2015. Hydrogen radiolytic release from zeolite 4A/water systems under γ irradiations. *Radiation Physics & Chemistry*, 110: 6–11.

Gan H.J., Xiao X.M., Lu Y.C., Jin Y.B., Tian H., and Liu D.H., 2007. Genetic relationship between natural gas dispersal zone and uranium accumulation in the northern Ordos Basin, China. *Acta Geologica Sinica* (English Edition), 81: 501–509.

Hou G.L., Liu C.W., Li R.Z., Xu H.G., Gao Y.Q., and Zheng W.J., 2017. Emergence of solvent-separated $Na^+$-$Cl^-$ ion pair in salt water: photoelectron spectroscopy and theoretical calculations. *Journal of Physical Chemistry Letters*, 8: 13–20.

Hu Q.Y., Kim, D.Y., Liu J., Yue M., Yang L.X., Zhang D.Z., Mao, W.L., and Mao H., 2017. Dehydrogenation of goethite in Earth's deep lower mantle. *PNAS*, 114: 1498–1501.

Hunt, J.M., 1996. *Petroleum geochemistry and geology (second edition)*. New York: Freeman.

Kelley, K.D., Karson, J.A., Blackman, R.K., Fruh-Green, G.L., Butterfield, D.A., Lillwy, M.S., Olson, E.J., Schrenk, M.O., Roe, K.K., Lebon, G.T., Rivizzigno, P., and the AT3-60 Shipboard Party, 2002. An off-axis hydrothermal vent field near the mid-atlantic ridge at 30 degrees N. *Nature*, 412: 145-149.

Kita, I., Matsuo, S., and Wakita, H., 1982. $H_2$ generation by reaction between $H_2O$ and crushed rock: An experimental study on $H_2$ degassing from the active fault zone. *Journal of Geophysical Research Solid Earth*, 87: 10789–10795.

Le, C.S., Rotureau, P., Brunet, F., Charpentier, T., Blain, G., Renault, J.P., and Mialocq, J.C., 2005. Radiolysis of confined water: hydrogen production at a high dose rate. *Chemphyschem*, 6: 2585–2596.

Li H.Y., 2000. A study of the accompanying relationships between uranium and oil. *Acta Geologica Sinica* (English Edition), 74: 595–601.

Li S.Y., Lin S.J., Guo S.H., and Liu L.F., 2002. Effects of inorganic salts on the hydrocarbon generation from kerogens, *Geochimica* 31:15-20 (in Chinese with English abstract).

Li X.Q., Hou D.J., Liu C.Q., and Zhang A.Y., 2001. The geochemistry characteristics of Ordovician formation water and dissolved gas of central gasfield in the Ordos Basin. *Fault-Block Oil & Gas Field*, 8: 1–6 (in Chinese with English abstract).

Li, J., and Chou, I. M., 2015, Hydrogen in silicate melt inclusions in quartz from granite detected with Raman spectroscopy. *Journal of Raman Spectroscopy*, 46: 983–986.

Liu C.Y., and Wu B.L., 2016. *Mineralization mechanism, spatial enrichment law of oil/gas coal and uranium coexisting in the same basin*. Beijing: Science Press (in Chinese).

Liu C.Y., Qiu X.W., Wu B.L., and Zhao H.G., 2007. Characteristics and dynamic settings of the Central-East Asia multi-energy minerals metallogenetic domain. *Science in China Series D-Earth Science*, 37: 1–15 (in Chinese with English abstract).

Liu Y.J., 2009. Crystallography. Xi'an: Northwest University Press (in Chinese with English abstract).

Lollar, B.S., Onstott, T.C., Lacrampe-Couloume, G., and Ballentine, C.J., 2014. The contribution of the precambrian continental lithosphere to global $H_2$ production. *Nature*, 516: 379-382.

Luo Y.R., 2005. Handbook of Bond Dissociation Energies in Organic Compounds. Beijing: Science Press (in Chinese).

Maeda, Y., Kawana, Y., Kawamura, Y., Hayami, S., Sugihara, S., and Okay, T., 2005. Hydrogen gas evolution from water included in a silica gel cavity and on metal oxides with γ-ray irradiation. *Journal of Nuclear & Radiochemical Sciences*, 6: 131–134.

Mao H., Hu Q.Y., Yang L.X., Liu J., Duck Y.K., Meng Y., Zhang L., Prakapenka, V.B., Yang W. and Mao, W.L., 2017. When water meets iron at Earth's core-mantle boundary. *National Science Review*, 0: 1–9.

Mapiour, M., Sundaramurthy, V., Dalai, A.K., and Adjaye, J., 2010. Effects of the operating variables on hydrotreating of heavy gas oil: experimental, modeling, and kinetic studies. *Fuel*, 89: 2536–2543.

Matar, S., and Hatch, L.F., 2001. *Chemistry of petrochemical processes (Second Edition)*. Houston: Gulf Publishing Company.

Miao J.Y., and Pang J.G., 2012. *Petroleum organic geochemistry*. Beijing: Petroleum Industry Press (in Chinese).

Musat, R.M., Cook, A.R., Renault, J.P., and Crowell, R.A., 2012. Nanosecond pulse radiolysis of nanoconfined water, Journal of Physical Chemistry, 116: 13104–13110.

Nakashima, M., and Masaki, N.M., 1996. Radiolytic hydrogen gas formation from water adsorbed on type Y zeolites. *Radiation Physics and Chemistry*, 47: 241–245.

Nakashima, M., and Tachikawa, E., 1987. Radiolytic Gas Production from Tritiated Water Adsorbed on Molecular Sieve 5A. *Journal of Nuclear Science and Technology*, 24: 41–46.

Olleta, A.C., Han, M.L., and Kim, K.S., 2006. Ab initio study of hydrated sodium halides NaX $(H_2O)_{1-6}$ (X=F, Cl, Br and I). *Journal of Chemical Physics*, 124: 024321–1–024321–13.

Ortiz, A.L., Zaragoza, M.J.M., and Collins-Martínez, V., 2016. Hydrogen production research in Mexico: a review. *International Journal of Hydrogen Energy*, 41: 23363–23379.

Pastina, B., and LaVerne, J., 2001. Effect of molecular hydrogen on hydrogen peroxide in water radiolysis. *Journal of Physical Chemistry A*, 105: 9316–9322.

Pastina, B., LaVerne, J.A., and Pimblott, S.M., 1999. Dependence of molecular hydrogen formation in water on scavengers of the precursor to the hydrated electron. *Journal of Physical Chemistry A*, 103: 5841–5846.

Potter, J., and Konnerup-Madsen, J., 2014. A review of the occurrence and origin of abiogenic hydrocarbons in igneous rocks. *Geological Society of London Special Publications*, 214: 151-173.

Qiu X.W., 2011. Characteristics and dynamic settings of Yanchang period hydrocarbon-rich depression in Ordos Basin, China: [*Dissertation*]. Xi'an, Northwest University (in Chinese with English abstract).

Rabiei, M., Chi, G., Normand, C., Davis, W.J., Fayek, M., and Blamey, N.J.F., 2018. Hydrothermal rare earth element (xenotime) mineralization at maw zone, Athabasca Basin, Canada, and its relationship to unconformity-related uranium deposits. *Economic Geology*, 112: 1483-1507.

Richard, A., 2017. Radiolytic ($H_2$, $O_2$) and other trace gases ($CO_2$, $CH_4$, $C_2H_6$, $N_2$) in fluid inclusions from unconformity-related U deposits. *Procedia Earth and Planetary Science*, 17: 273-276.

Rong C.F., 2002. *Ionizing radiation dose*. Beijing: Atomic Energy Press (in Chinese).

Schrenk, M.O., Brazelton, W.J., and Lang, S.Q., 2013. Serpentinization, carbon, and deep life. *Reviews in Mineralogy & Geochemistry*, 75: 575–606.

Seewald, J.S., 2003. Organic-inorganic interaction in petroleum-producing sedimentary basins. *Nature*, 426: 327–333.

Sugisaki, R., and Sugiura, T., 1986. Gas anomalies at three mineral springs and a fumarole before an inland earthquake, Central Japan. *Journal of Geophysical Research Solid Earth*, 91: 12296–12304.

Tan C.O., Liu C.Y., Zhao J.L., and Zhang R.R., 2007. The radioactive abnormality characteristics of typical regions in Ordos Basin and its geological implications. *Science in China Series D: Earth Science*, 50: 174–184.

Tissot, B.P., and Welte, D.H., 1978. Petroleum formation and occurrence-A new approach to oil and gas exploration. Berlin: Springer Verlag.

Truche, L., Joubert, G., Dargent, M., Martz, P., Cathelineau, M., Rigaudier, T., and Quirt, D., 2018. Clay minerals trap hydrogen in the Earth's crust: Evidence from the Cigar Lake uranium deposit, Athabasca. Earth and Planetary Science Letters, 493: 186-197.

Veras, T.D.S., Mozer, T.S., and César, A.D.S., 2017. Hydrogen: trends, production and characterization of the main process worldwide. *International Journal of Hydrogen Energy*, 42(4): 2018–2033.

Wakita, H., Nakamura, Y., Kita, I., Fujii, N., and Notsu, K., 1980. Hydrogen release: new indicator of fault activity. *Science*, 210: 188–190.

Wang W.Q., Liu C.Y., Wang J.Q., Ma H.H., and Guan Y.Z., 2018. Characteristics of uranium content and its geological and mineralization significance for the provenance areas, Northwest China. *Earth Science Frontiers*, 26: 292-303 (in Chinese with English abstract).

Wang X.B., Tuo J.C., Zhou S.X., Li Z.X., and Yan H., 2005. Organic matter evolution and oil-gas resource in deep Earth. *Petroleum exploration and development*, 32: 159–164 (in Chinese with English abstract).

Wang X.F., Liu W.H., Xu Y.C., Zheng J.J., and Zhang D.W., 2006. Thermal simulation experimental study on the effect of water on the formation of gaseous hydrocarbons in organic matters. *Progress in Natural Science*, 16: 1275–1281 (in Chinese with English abstract).

Zhang D.X., and Gao J.S., 1996. The effect of co-hydrogenation of petroleum heavy oil and coal on heavy oil properties. *Petrochemical Technology*, 25: 466–470 (in Chinese with English abstract).

Zhang K., Liu T., Dai L.S., and Nie H., 2012. Study on the variations of hydrotreating reactions for recycal oil. *Petroleum Processing and Petrochemicals*, 43: 5-9 (in Chinese with English abstract).

Zhang W.Z., Yang H., Yang Y.H., Kong Q.F., and Wu K., 2008. Petrology and element geochemistry and development environment of Yanchang Formation Chang-7 high quality source rocks in Ordos Basin, *Geochimica* 37: 59–64 (in Chinese with English abstract).